Molecular Crystals and Liquid Crystals
Publication details, including instructions for authors and subscription information:
http://www.tandfonline.com/loi/gmcl16

Heat Pulses in Molecular Solids: Phonon-induced delocalization of trapped excited triplet states

A. R. Burns [a] [b] & C. B. Harris [a] [b]

[a] Department of Chemistry and Materials and Molecular Research Division of the Lawrence Berkeley Laboratory, University of California, Berkeley, California, 94720, U.S.A.

[b] Department of Chemistry, University of California, Los Angeles, California, 90024, U.S.A.

To cite this article: A. R. Burns & C. B. Harris (1980): Heat Pulses in Molecular Solids: Phonon-induced delocalization of trapped excited triplet states, Molecular Crystals and Liquid Crystals, 58:1-2, 1-18

To link to this article: http://dx.doi.org/10.1080/01406568008070147

Mol. Cryst. Liq. Cryst., 1980, Vol. 58, pp. 1–18
0026-8941/80/5801-0001$04.50/0

Printed in U.S.A.

Heat Pulses in Molecular Solids

Phonon-induced delocalization of trapped excited triplet states

A. R. BURNS† and C. B. HARRIS

Department of Chemistry and Materials and Molecular Research Division of the Lawrence Berkeley Laboratory, University of California, Berkeley, California 94720, U.S.A.

Thermal modulation spectroscopy is used to analyze the dynamics of energy redistribution between trap states and band states in the one-dimensional exciton system 1,2,4,5-tetrachlorobenzene. The time-resolved decrease in the phosphorescence intensity emitted from localized or "trapped" excited states in 1,2,4,5-tetrachlorobenzene (TCB), which occurs during the propagation time of a 1.0 msec heat pulse, is analyzed in terms of the direct absorption of phonons resonant with the trap depth. For each of the three traps studied, the heat pulse power dependence of the phosphorescence change can be related to the power dependence of the resonant phonon flux radiated by the heater. The data demonstrates that (i) single phonon events are probably responsible for the promotion of the trap state to the band state (ii) the redistribution of the excitation energy into the bands exhibits an explicit dependence of the density of states function and (iii) the extent of the trap state depletion is shown to be sensitive to the nature of the trap.

I. INTRODUCTION

Energy migration in ideal molecular crystals can be discussed in terms of the exciton theory formulated by Frenkel[1] and Davydov.[2] In any real crystal, however, there are always finite quantities of imperfections incorporated into the lattice. In many cases, the imperfections give rise to new excited states which are effectively removed from the band.[3] When these localized states are lower in energy than the exciton band, they can act as "traps." The exchange of energy between the host molecules comprising the band and those molecules which give rise to the trap states requires the intervention of a lattice phonon to make up the energy difference between the two levels (Figure (1)). A complete dynamical picture of energy migration in molecular

---

† Present address: Department of Chemistry, University of California, Los Angeles, California, 90024, U.S.A.

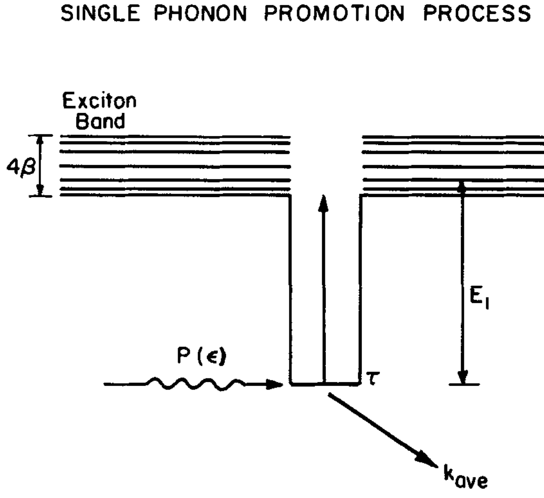

FIGURE 1 Kinetic model for the single phonon-assisted promotion of a localized trap state to a state isoenergetic with the exciton band. The energy E of the phonon P is resonant with the trap depth E_l. The width of the exciton band 4β (1.3 cm^{-1}) is a function of the intermolecular interaction energy.[4] The spectroscopic trap depth Δ (not shown) is in relation to the top of band ($k = 0$). Thus the energy range of the resonant phonons is $(\Delta - 4\beta) \to \Delta$. The average radiative rate constant of the three triplet sublevels is given by k_{ave}.

solids must include a description of the mechanism by which the phonon-mediated transfer takes place.

The probability that a phonon (or phonons in the case of a multiphonon process) of sufficient energy will induce a trap-to-band promotion will be a function of the density of band states and will be sensitive to the coupling of the trap state with the phonon.[4] The latter feature is expected to be affected by the intrinsic nature of the trap state, e.g., mechanical defects (x-traps), chemical impurities (y-traps), or isotopic.[5]

The rates of thermal trap-to-band promotion of excited triplet state energy in 1,2,4,5-tetrachlorobenzene (TCB) were measured by the methods of spin coherence[4,6] and pulsed dye laser excitation.[7] In both sets of experiments, it was shown that for dilute trap concentration ($<1\%$), the temperature dependence of the promotion rate yielded an activation energy which was equal to the "trap depth." Francis and his co-workers[8,9] demonstrated that the phosphorescence intensity of trap emission and exciton emission can be modulated by the application of a millisecond heat pulse from a small heater in thermal contact with a TCB crystal.

Ideally, the most direct way of studying phonon interactions in crystals is to artificially generate the resonant phonons. High frequency phonons with energies exceeding 30 cm^{-1} or more can be produced by the Joule heating of thin films.[10,11] The central frequency in the heat pulse spectrum is proportional to kT_H/h, where T_H is the heater temperature. The heat pulse technique has the disadvantage, however, of employing a very broad band source of phonons, since the width about the central maximum is also proportional to kT_H/h. Despite this undesirable feature, it can be shown that if the phonon absorption and/or scattering processes under question are frequency selective, then the coupling of a broad band source to a crystalline sample can yield the same information as that obtained with a monochromatic phonon source (such as a superconducting tunnel-junction).

The purpose of this paper will be to demonstrate the feasibility of probing phonon interactions in molecular crystals by way of the heat pulse technique. Specifically, the trap-to-band promotion process occurring in the single x-trap system[4] in neat h_2-TCB and the multiple isotopic hd and h_2 trap system in d_2-TCB will be studied. By comparing the extent of trap-to-band promotion via the heat pulse in both systems, one can begin to answer questions regarding the frequency selectivity of the process, as well as the dependence of the process on the density of band states and the nature of the trap.

II. THEORY

Most of the experimental work since the advent of heat pulses in solids[10,11] has been concerned with the ballistic propagation of high frequency acoustic phonons in the nanosecond time scale. In these experiments, the thermal coupling of the phonon source and the transmission medium is maximized by the direct vacuum evaporation of the heater film on to the crystal surface. A notable exception is found in the work of Broude *et al.*,[12,13] who generated nanosecond pulses in anthracene crystals by the heat release following optical excitation. Unfortunately, there presently does not exist a feasible way of depositing stable heater films on fragile, low-melting point materials such as molecular crystals. Thus, in order to attempt the experiments, one must bond the crystals to a heater film which is vacuum evaporated on another substrate. (It is still advantageous to use a thin film, 1000 Å thick, in order to insure a rapid heating of the source). The relatively poor thermal contact between the crystal surface and the heating film precludes a time resolution on the nanosecond time scale; hence, one cannot detect the propagation of a short pulse of phonons. However, as evidenced by the work of Francis,[8,9] one can detect the absorption of phonons produced by heat pulses which are much longer (msec) than the inherent transit time of the phonons in the crystal.

Even though the thermal boundary conductance between the crystal and the heater may be poor, it is possible that the phonons that do propogate through the crystal will have a frequency spectrum which is characterized by the temperature of the heater film. A completely analogous experiment was reported by Anderson and Sabisky,[14] who demonstrated that changes in the spin populations in a $SrF_2:Tm^{+2}$ crystal could be used to analyze the spectrum of the phonons coming from a heating wire which was glued to the crystal. The electrical current to the heater was modulated on and off at 20 Hz. The authors proceeded to show that the frequencies of the phonons absorbed by the spin system could be related to the same effective heater temperature.

The energy lost per unit time from a unit area A of the heater is proportional to the thermal conductance away from the heater and the fourth power of its temperature, T_H :[15,16]

$$\frac{P}{A}(T_H, T_B) = \sigma(T_H^4 - T_B^4) \tag{1}$$

$$\sigma = \frac{\pi^5 k^4 \Gamma}{5 v_H^2 h^3} \tag{2}$$

This relationship is completely analogous to the Stefan–Boltzmann law for the thermal radiation of photons. In this case, σ is equivalent to the Stefan–Boltzmann constant, v_H is the average velocity of sound in the black body source, and T_B is the ambient temperature. The transmission coefficient Γ is a function of the acoustic mismatch between the heater and the crystal. From the acoustic mismatch theory of Little,[17] it can be shown that the net flux of phonons of all polarizations with frequency ν from the heater at a temperature T_H is given by:

$$\frac{N(\nu, T_H, T_B)}{A} = \frac{6\pi\Gamma\nu^2}{v_H^2}\left[\frac{1}{\exp(h\nu/kT_H) - 1} - \frac{1}{\exp(h\nu/kT_B) - 1}\right] \tag{3}$$

Eq. (3) can be rewritten in terms of σ in Eq. (2):

$$N(\nu, T_H, T_B) = \frac{30h^3\nu^2\sigma}{\pi^4 k^4}\left[\frac{1}{\exp(h\nu/kT_H) - 1} - \frac{1}{\exp(h\nu/kT_B) - 1}\right] \tag{4}$$

If there are no thermal losses from the heater other than through the crystal interface, then the total radiated acoustic power in Eq. (1) will be equal to the electrical power dissipated in the heater. However, since the heater is a film supported by another substrate (see Figure (2) in Sec. III), and since the heater/crystal assembly is totally immersed in liquid He, there are additional routes for thermal losses. Therefore, one is required to formulate a proportionality constant B, which incorporates all radiative losses, such that an "effective" heater temperature T_{HE} can be calculated from the input power P_i:

$$T_{HE} = \left(\frac{P_i}{BA} + T_B\right)^{1/4} \tag{5}$$

The effective temperature of the heater is thus a function of the energy balance between the input electrical power and the phonon radiation to the surrounding media.

The phonon flux presented in Eq. (4) can then be rewritten in terms of the effective heater temperature T_{HE} and the proportionality constant B:

$$\frac{N(\nu, T_{HE}, T_B)}{A} = \frac{30h^3\nu^2 B}{\pi^4 k^4}\left[\frac{1}{\exp(h\nu/kT_{HE}) - 1} - \frac{1}{\exp(h\nu/kT_B) - 1}\right] \tag{6}$$

If one assumes that the thermal promotion process involves a single phonon, then a trap state with an energy $(\Delta - 4\beta)$ below the bottom of the exciton band, which has a width 4β, will be promoted to an intermediate state isoenergetic with the band by the absorption of phonons having energies in the range $(\Delta - 4\beta) \to \Delta$. The integration of Eq. (6) over the limits of this frequency range will yield the resonant phonon flux $F(P_i)$ for an input power P_i:

$$F(P_i) = \frac{1}{A}\int_{\nu_l}^{\nu_h} N(\nu, T_{HE}, T_B)\,d\nu, \tag{7}$$

where

$$\nu_l = \frac{\Delta - 4\beta}{h}, \tag{8}$$

and

$$\nu_h = \frac{\Delta}{h} \tag{9}$$

Eq. (7) can be evaluated for given values of B, P_i, T_B, ν_h and ν_l by using Simpson's approximation (continuous). One can now define an "absorption coefficient" ϕ as the ratio of the relative modulation depth of the trap population to the resonant phonon flux:

$$\phi \equiv \frac{(\Delta n_{\max}/n_{ss})}{F(P_i)}, \tag{10}$$

where $\Delta n_{\max}$ is the maximum change in the trap population relative to the steady-state population n_{ss} at temperature T_B.

Since the intensity of the phosphorescence emission from the trap is equal to the product of the trap population and the temperature—independent radiative rate constant, Eq. (10) may be rewritten in terms of the relative trap phosphorescence modulation depth:

$$\phi = \frac{(\Delta I_{\max}/I_{ss})}{F(P_i)} \tag{11}$$

The value of ϕ is not a true absorption coefficient in a spectrophotometric sense, but merely serves the purpose of normalizing the modulation depths found for a series of different crystals having various traps and trap concentrations.

From Eq. (5), a set of effective heater temperatures can be calculated for a given power range and proportionality constant B. This set of T_{HE} values can then be substituted into Eq. (7) in order to generate the power dependence of the phonon flux $F(P_i)$, which is resonant with a particular trap-to-band promotion. In the absence of saturation, spin-lattice relaxation between the triplet sublevels of the trap state, and direct trap-to-trap energy transfer, the relative phosphorescence modulation depth should have the same power dependence as the resonant phonon flux. Unfortunately, the proportionality constant B is not known *a priori.* It is difficult, therefore, to predict what the resulting power dependence of $\Delta I_{\max}/I_{ss}$ will be for a particular trap promotion. However, from the *observed* power dependence of $\Delta I_{\max}/I_{ss}$, the parameter B can be determined by finding that value which produces the identical phonon flux power dependence. If one prepares a series of crystals, each having the same host material, but containing various concentrations of traps, and then places the crystals individually on the same heater film, then the only expected change in B from experiment to experiment should be due to the somewhat variable heater/crystal boundary conductance. Since the changes of this nature in B will be taken into account in the calculation of the resonant phonon flux, a valid comparison of ϕ can be made for the different trap-band systems.

There are two more considerations that must be brought up at this time. The first consideration is that of scattering of the generated phonons in the crystal itself. With the exception of the work by Broude,[12,13] there has been very little reported work on the thermal conductivity of molecular crystals at low temperatures ($T_B < 4.2$ K). At low temperatures, one does not expect phonon-phonon scattering (Umklapp processes) to be important.[18–20] Point defect scattering may be significant, however. If the crystals are grown from exceptionally clean material, then isotopic scattering is expected to dominate. Walter and Pohl[21] found that the total isotopic scattering rate of a phonon with frequency v is given by

$$k = \left(\frac{4\pi^3 V_0 s}{v^3}\right) v^4, \tag{12}$$

where

$$s = \sum f_i \left(\frac{1 - m_i}{\bar{m}} \right)^2 \tag{13}$$

V_0 is the molecular volume, v is the velocity of sound, $\bar{m}$ is the average molecular mass, and f_i is the relative concentration of mass m_i. From the analysis of the mass spectrum of each crystal,[22] the value for s was not found to exceed 6.8×10^{-5}. The velocity of sound in TCB is roughly 1.6×10^5 cm/sec.[22] Hence the isotopic scattering rate should not exceed $4 \times 10^{-40} \nu^4 \text{ sec}^{-1}$ for the crystals under study. For a typical sample thickness L of 0.04 cm, the boundary scattering rate (v/L) is about $4.0 \times 10^6 \text{ sec}^{-1}$. In order for the isotopic scattering rate to be comparable to that of boundary scattering, the phonon frequency must exceed $3.2 \times 10^{11} \text{ sec}^{-1}$, which is equivalent to an energy of 11 cm^{-1}. Since the trap depths for crystals studied here range from 11 cm^{-1} to 22 cm^{-1}, it is possible that many of the phonons will be isotopically scattered before they reach the crystal/bath boundary.

The second consideration that must be taken into account is the thermal coupling of the crystal to the surrounding superfluid He bath. A bottleneck at the crystal/bath boundary may result in the "overheating" of the crystal sample. However, it has been shown in many previous investigations[23–25] that solid material/liquid He boundary conductances for high frequency phonons (10^{11} sec^{-1}) are much higher than those predicted by acoustic mismatch theory. Evidence that this also appears to be the case in this set of experiments will be presented in Sec. IV.

III. EXPERIMENTAL

Highly purified h_2-TCB (1,2,4,5-tetrachlorobenzene) was prepared by zone-refining through 1400 or more passes re-crystallized, reagent grade material. No signs of chemical impurities (e.g., y-traps) were evident in the phosphorescence spectrum, and strong exciton emission was observed at temperatures as low as 2.0 K. Perdeuterated TCB was synthesized by the Fooladi method.[26] Following deuteration, the material was extensively zone-refined. Higher concentrations of h_2-TCB were incorporated by adding small amounts to the d_2-TCB material just before the crystals were grown. Each crystal was grown from the melt in a Bridgman furnace,[27] and later annealed for ten days at 138°C.

The experimental arrangement is shown in Figure (2). Each neat h_2-TCB and d_2-TCB sample was cut from a single crystal along the principal cleavage planes (001) into a slab having a cross-sectional area of 6 mm^2 and a typical thickness of 0.4 mm. The sample was bonded with a very thin layer of Dow

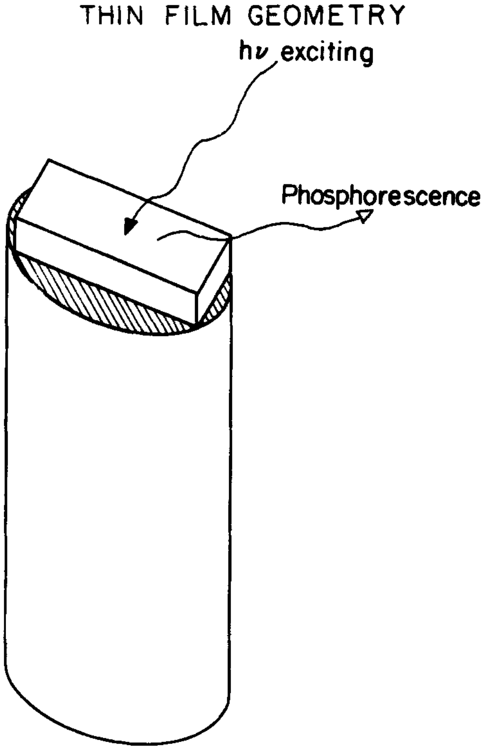

FIGURE 2 Heater/crystal arrangement for the optical detection of phosphorescence changes due to heat pulse propagation. The emission from the surface of the crystal is detected at 90° from the exciting light. The crystal actually covers the entire heater film, which is exposed here to facilitate display. The heater is a thin film (1000 Å) of nichrome vacuum evaporated on to the quartz rod (3 mm diam.) substrate. Not shown are the thin film gold strips on opposite sides of the quartz rod which provide electrical contact to the 50 Ω nichrome film.

silicone grease to a heater film which was used in all the experiments. The heater/crystal assembly was inserted in a cryostat and totally immersed in liquid He. The temperature of the bath was controlled by a pressure regulator in a mechanical pumping line and monitored by a calibrated germanium thermistor.

Each sample was excited into the upper singlet state manifold by a 100 W high pressure Hg lamp filtered at 2800 Å. The subsequent phosphorescence from the first excited triplet state was detected at 90° with a $\frac{3}{4}$ meter Jarrell–Ash Czerny–Turner monochromator, equipped with an EMI 6256S photomultiplier. The emission from the 17.3 cm^{-1} x-trap in neat h_2-TCB and the emission from the 11.1 cm^{-1} hd-TCB and 21.6 cm^{-1} h_2-TCB traps in d_2-TCB are easily resolved with respect to the exciton lines, both at the electronic origin and the b_{2g} vibronic origin.[6,28,29]

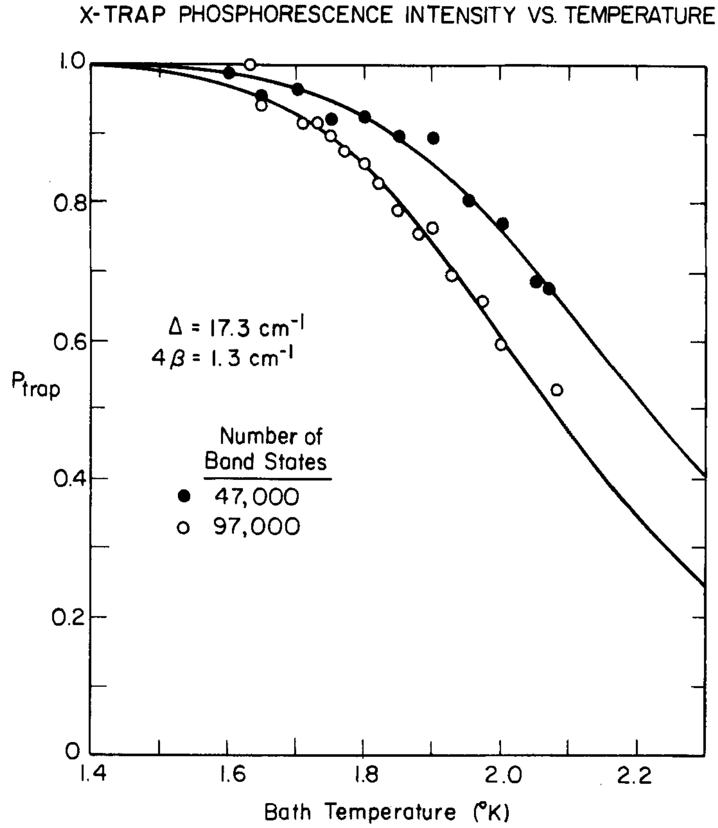

FIGURE 3 Bath temperature dependence of the x-trap phosphorescence intensity for two different neat h_2-TCB crystals. The number of exciton band states in each crystal is found by fitting the normalized data points to curves calculated from Boltzmann statistics when the spectroscopic trap depth Δ and the exciton band width 4β are known.

The temperature dependences of the x-trap phosphorescence intensity for two neat h_2-TCB crystals are shown in Figure (3). Since the triplet energy in the neat h_2-TCB crystal is partitioned between the x-trap and the exciton band states, Boltzmann statistics can be used to determine the number of band states, and hence the concentration of x-traps, from the phosphorescence intensity temperature dependence. The two curves shown in Figure (3) are the best fits to the normalized trap intensities; details concerning this analysis can be found in Refs. 4, 7, and 29. One can see that the x-trap concentrations in these crystals are less than one part in 10^4. The temperature dependences of two d_2-TCB crystals are shown in Figure (4). In d_2-TCB crystals containing concentrations of h_2-TCB above 1 %, the phosphorescence emission is almost exclusively from the deeper h_2-TCB trap.

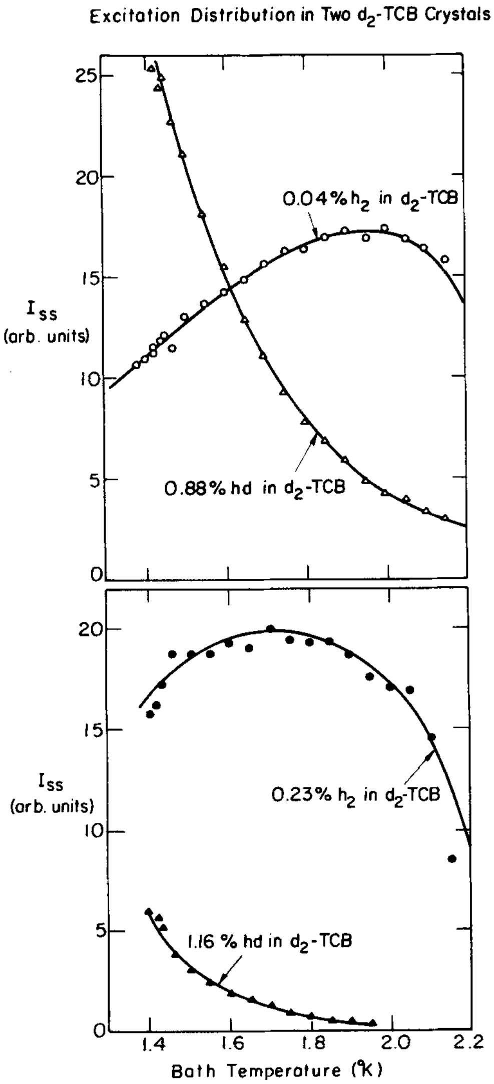

FIGURE 4 Non-Boltzmann bath temperature dependence of the excitation distribution between the *hd* (11 cm^{-1}) and the h_2 (22 cm^{-1}) isotopic traps in two d_2-TCB crystals. White circles and triangles: 99.1% d_2-TCB. Black circles and triangles: 98.6% d_2-TCB.

The heat pulse-induced phosphorescence modulation was carried out as follows. An electronic shutter was placed in front of the monochromator's entrance slits so that the dark level of the photomultiplier could be established. The shutter was triggered to open for 1/15th of a second at a repetition rate of 4.5 Hz. After a delay time suitable to establish the level of the steady state phosphorescence intensity I_{ss} (i.e. when the shutter was completely open), a 1.0 msec current pulse from a Rutherford B-78 generator was dissipated at the heater film. The resulting signal, as shown in Figure (5), was averaged 512 times or more on a Northern NS-575 multichannel analyzer. In the case of trap phosphorescence modulation, $\Delta I_{\max}$ was a negative change in light intensity; whereas in the case of exciton phosphorescence modulation, $\Delta I_{\max}$ was a positive change in light intensity. All the pulse voltages across the 50Ω heater film were monitored on a Tektronix 454 oscilloscope. The rise time of the current pulse was 10 μsec or less, while the rise time of the phosphorescence modulation τ_R (Figure (5)) was generally 0.3 msec and bath temperature-independent.

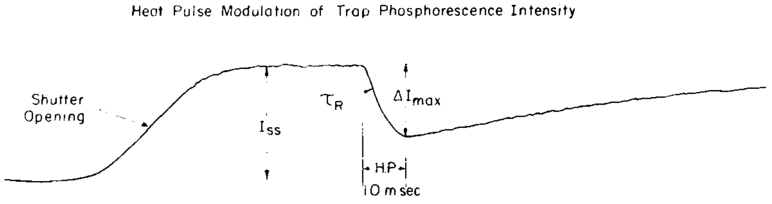

FIGURE 5 Time-resolved heat pulse modulation of trap phosphorescence intensity obtained by signal averaging. The steady-state intensity I_{ss} is established by opening a shutter which is in front of the monochromator. The modulation depth $\Delta I_{\max}$ always coincides with the end of the heat pulse. The rise time of the phosphorescence change τ_R is usually about 0.3 msec for a 1.0 msec pulse. The much longer recovery time (30 msec) of the trap population after the heat pulse is due to the slow feeding rate following electronic excitation.

IV. RESULTS AND DISCUSSION

Examples of the phosphorescence modulation power dependence for each of the three traps are shown in Figure (6). The curves drawn through the data points yield the respective power dependences which are used to calculate the resonant phonon fluxes. One immediately notices that the x-trap $\Delta I_{\max}/I_{ss}$ values are significantly lower than either of the two isotopic trap values, even though the depth of the x-trap is in between the depth of the hd-TCB trap and depth of the h_2-TCB trap. Furthermore, the density of band states in neat h_2-TCB is nearly three orders of magnitude higher than that in the d_2-TCB crystals. The values of $\Delta I_{\max}/I_{ss}$ for the shallow hd-TCB trap are

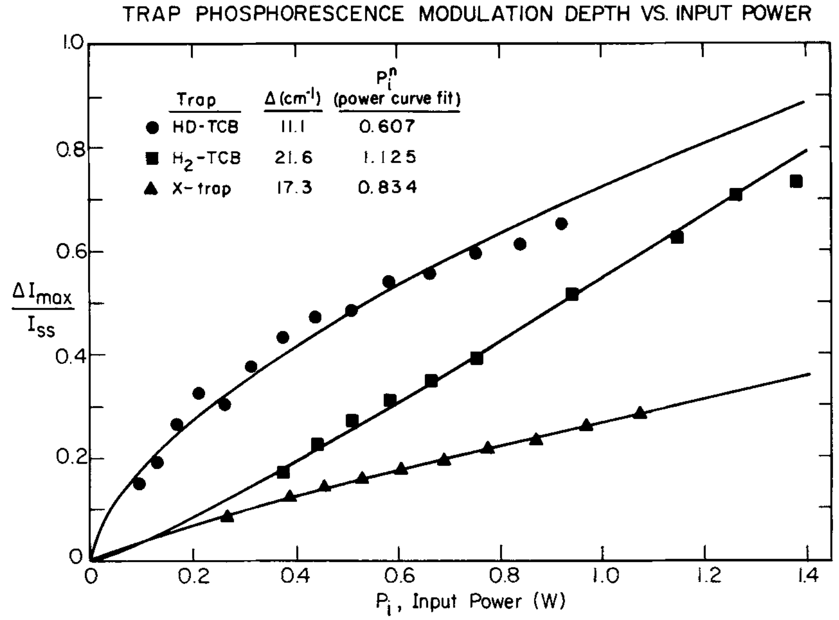

FIGURE 6 Power dependence of the relative modulation depth for three traps in TCB. The x-trap is in neat h_2-TCB and the isotopic traps, hd and h_2-TCB, are in d_2-TCB. The input power P_i is over an interfacial area of 6 mm^2.

clearly greater at a given input power than those for the deep h_2-TCB trap in the same d_2-TCB crystal. This is what one expects, however, since the flux of phonons resonant with the 11 cm^{-1} hd trap is greater than that of the higher frequency modes resonant with the 22 cm^{-1} h_2 trap. Since the extent of depletion of each trap has a unique power dependence which is a function of the trap depth Δ, *it appears that the thermal promotion process in these systems is a single phonon event.*

The power dependences of the corresponding exciton phosphorescence modulation depths follow that of the traps only at low input powers ($P < 0.01$ W/mm). At higher powers, bi-exciton annihilation distorts the power dependence in the neat h_2-TCB crystals. This effect was also observed by Francis.[9] In the d_2-TCB crystals, the low-power increases in the exciton emission are predominately due to the promotion of the hd trap population. As the power is increased, the simultaneous depletion of the deep h_2 trap distorts the power dependence of the exciton modulation depth. Thus all the results presented here will be those obtained from the trap modulation data.

In Table I, the results are shown for the phonon flux analyses of the x-trap phosphorescence modulation in three neat h_2-TCB crystals. From at least eight different input powers in the given range, the observed modulation

TABLE I

Phosphorescence modulation of x-traps in h_2-TCB $\Delta = 17.3\ \mathrm{cm}^{-1}$, $4\beta = 1.3\ \mathrm{cm}^{-1}$

Sample	P_i range (W/mm^2)	P_i dependence	B (mW/cm^2-K^4)	T_{HE} range (K)	$\phi \times 10^{-18}$	Band States ± 3000
A, 2.0 K	0.032–0.315	0.741	2.5	6.02–10.6	1.722 ± 0.037	86,000
B, 2.0 K	0.047–0.367	0.900	7.2	5.09–8.46	1.469 ± 0.058	50,000
C, 2.0 K	0.045–0.180	0.834	3.7	5.93–8.38	0.923 ± 0.016	47,000
C,[a] 2.0 K	0.055–0.162	0.852	4.0	6.10–7.98	0.922 ± 0.019	47,000
C, 1.75 K	0.045–0.180	0.868	4.0	5.81–8.20	0.772 ± 0.062	47,000
C,[a] 1.75 K	0.045–0.180	0.909	5.0	5.50–7.75	0.746 ± 0.022	47,000
C, 1.48 K	0.055–0.180	0.754	2.5	6.85–9.21	0.805 ± 0.018	47,000
C,[a] 1.48 K	0.045–0.180	0.852	3.7	5.92–8.37	0.706 ± 0.008	47,000

[a] b_{2g} emission.

depth power dependence is determined. Each value of the black body proportionality constant B is then determined by that value which generates a phonon flux having the identical power dependence in the energy range 16.0–17.3 cm^{-1} (see Eq. (7)). The corresponding effective heater temperatures T_{HE} for the given power range B are also tabulated. The values for the heater temperatures are very consistent from one experiment to the next. In the case of sample B, Apiezon N grease was used between the crystal and the heater; thus it appears that the proportionality constant B is sensitive to changes in the thermal conductance of the grease-mediated heater/crystal interface.

The most noteworthy feature in Table I is that the value of ϕ, which represents the normalization of trap modulation depth with respect to the resonant phonon flux, varies directly with the number of available band states. *Thus the net transfer of energy from the localized state to the set of delocalized band states increases with density of band states.*

In order to see if the phosphorescence modulation monitored at the electronic origin (3751 Å) was due solely to promotion of trapped population to the band, the emission to the b_{2g} vibronic origin (3781 Å) was also monitored. It has been shown previously[28] that there exists a non-Boltzmann spin distribution among the triplet sublevels of the trap states. When the trap state is far removed from the band (e.g., the 1400 cm^{-1} TCB trap in durene), the thermal modulation of the trap phosphorescence is due only to changes in the spin distribution,[8] *via* spin lattice relaxation. However, when the trap state is only 17 cm^{-1} lower in energy than the band, one expects that the thermal promotion process will dominate over the much slower spin lattice relaxation process. This notion is borne out in these experiments by the observation that the modulation depth of the x-trap b_{2g} emission is identical, within experimental error, to that monitored at the electronic origin. Since the emission at the electronic origin comes from a different triplet sublevel than that which gives rise to the emission at the b_{2g} vibronic origin, one can conclude that the phosphorescence modulation is due only to trap-to-band promotion.

The phosphorescence modulation results for the *hd* and h_2 traps in d_2-TCB are shown in Tables II and III, respectively. The resonant phonon fluxes for the *hd*-TCB trap are calculated for the energy range of 9.8–11.1 cm^{-1}; whereas the resonant phonon fluxes for the h_2-TCB trap are calculated for the energy range of 20.3–21.6 cm^{-1}. Due to the large amount of scatter in each of the last six h_2-TCB trap power dependences in Table III, the calculated fluxes had to be extrapolated with the average value of B found for all the previous experiments (x-trap, *hd*, and h_2). The error in this average value ($B = 4.5 \pm 1.9$ $\text{mW/cm}^2\ \text{K}^4$) is included in the error for ϕ. Despite the lack of precise curve-fitting, there is a definite trend of a decreasing absorption coefficient with the reduction in the number of host d_2-TCB molecules.

When one compares the absorption coefficients of the *hd* and h_2 traps, one can see that the *hd* values are somewhat smaller than the h_2 values. A frequency dependence for the phonon-mediated promotion process is not expected. The discrepancy may more likely be due to a preferential energy transfer from the deep h_2 trap to the shallow *hd* trap during the course of the heat pulse. The energy migration can take place either indirectly via the exciton band or by direct trap-to-trap transfer.[5] In any case, the absorption coefficients for the two isotopic traps are appreciably greater than those found for the x-trap in neat h_2-TCB. The results thus indicate *that the thermal promotion of the x-trap involves a less effective phonon coupling of the localized state to the band.*

Due to the relatively high effective heater temperatures, the bath temperature makes almost no contribution to the calculated flux of resonant phonons. In Figure (7), the results are shown for the bath temperature dependence of $\Delta I_{\text{max}}/I_{ss}$ for the x-trap in neat h_2-TCB. At bath temperatures below 2.1 K, the phosphorescence modulation is constant to within 3 %. The rate of repopulating the traps following the heat pulse (Figure (5)) is also constant below 2.1 K. However, when the bath temperature approaches the lambda-point of liquid He, a dramatic change in the thermal coupling of the heater/crystal assembly to the bath takes place. Not only does the modulation depth $\Delta I_{\text{max}}/I_{ss}$ increase steeply, but also the rate of trap repopulation decreases significantly. Thus it appears that the crystal is being "saturated" with phonons resonant with the trap depth due to the loss of thermal coupling between the crystal and the He bath. Since the heater/crystal interface is permeated with superfluid He, the rise time τ_R of the phosphorescence modulation also increases somewhat. Similar liquid He effects have been observed by Buckley,[30,31] and Glättli.[32] An important conclusion that can be drawn from this

TABLE II

Phosphorescence modulation of *hd*-traps in d_2-TCB $\Delta = 11.1\ \mathrm{cm}^{-1}$, $4\beta = 1.3\ \mathrm{cm}^{-1}$

Sample	Trap conc.	P_i range (W/mm^2)	P_i dependence	B (mW/cm^2-K^4)	T_{HE} range (K)	$\phi \times 10^{-18}$	*Host molecules/* trap
D, 2.0 K	1.16 % *hd*, 0.23 % h_2	0.016–0.16	0.607	3.5	4.64–8.12	2.115 ± 0.079	72
E, 1.7 K	0.88 % *hd*, 0.04 % h_2	0.028–0.06	0.578	2.3	5.91–7.17	2.58 ± 0.05	110
E, 1.45 K	0.88 % *hd*, 0.04 % h_2	0.028–0.11	0.679	6.0	4.67–6.55	2.54 ± 0.10	110
F, 1.50 K	0.88 % *hd*, 0.04 % h_2	0.011–0.14	0.735	6.0	3.68–6.93	2.32 ± 0.18	110

TABLE III

Phosphorescence modulation of h_2-traps in d_2-TCB $\Delta = 21.6\ \mathrm{cm}^{-1}$, $4\beta = 1.3\ \mathrm{cm}^{-1}$

Sample	Trap conc.	P_i range (W/mm^2)	P_i dependence	B (mW/cm^2-K^4)	T_{HE} range (K)	$\phi \times 10^{-18}$	*Host molecules/* trap
D, 2.0 K	1.16 % *hd*, 0.23 % h_2	0.063–0.230	1.125	6.3	5.63–7.77	2.55 ± 0.076	72
D, 1.70 K	1.16 % *hd*, 0.23 % h_2	0.140–0.230	1.129	9.3	6.23–7.05	2.74 ± 0.13	72
E, 1.80 K	0.88 % *hd*, 0.04 % h_2	0.147–0.207	0.964	4.8	7.43–8.09	3.46 ± 0.12	110
E, 1.70 K	0.88 % *hd*, 0.04 % h_2	0.147–0.207	0.95[a]	4.5 ± 1.9	7.5–8.2	3.08 ± 0.34	110
E, 2.0 K	0.88 % *hd*, 0.04 % h_2	0.139–0.207	0.96[a]	4.5 ± 1.9	7.4–8.2	2.56 ± 0.26	110
G, 1.50 K	1.42 % *hd*, 0.78 % h_2	0.067–0.193	1.07[a]	4.5 ± 1.9	6.2–8.1	1.17 ± 0.14	42
G, 2.00 K	1.42 % *hd*, 0.78 % h_2	0.102–0.176	1.02[a]	4.5 ± 1.9	6.9–7.9	1.89 ± 0.52	42
H, 1.5 K	1.6 % *hd*, 5.4 % h_2	0.067–0.114	1.13[a]	4.5 ± 1.9	6.2–7.1	0.94 ± 0.18	14
H, 2.0 K	1.6 % *hd*, 5.4 % h_2	0.067–0.143	1.09[a]	4.5 ± 1.9	6.2–7.5	0.83 ± 0.16	14

[a] Average power dependence obtained with extrapolated $B = 4.5 \pm 1.9$ mW/cm^2-K^4 (T_{HE} is also obtained from extrapolated B).

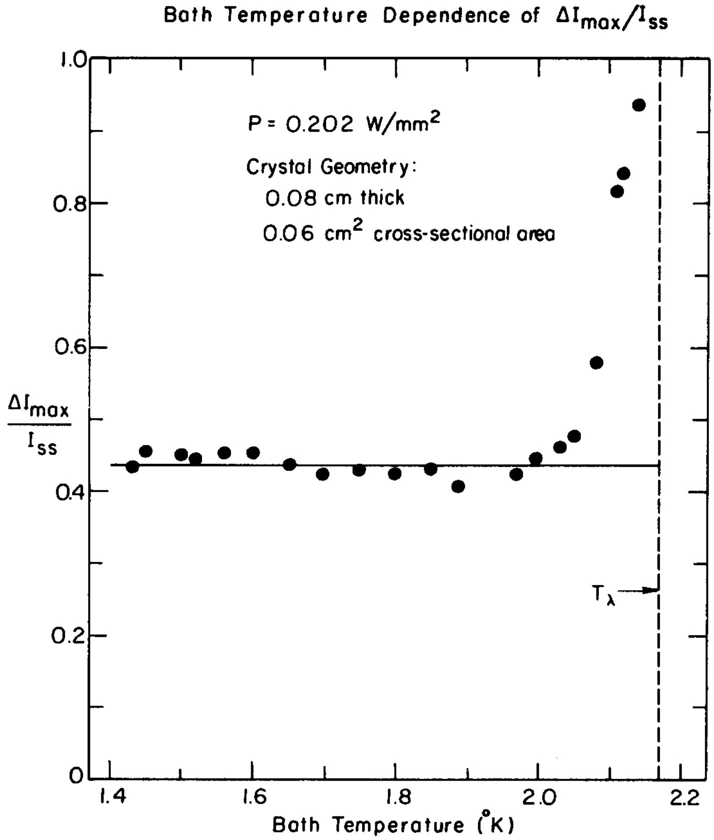

FIGURE 7 Bath temperature dependence of the relative modulation depth at a constant input power of 0.202 W/mm^2. The straight line drawn through the points taken below 2.1 K is the average value of 0.435 ± 0.014. The rapid rise in the modulation depth near the lambda point is a liquid He effect.

experiment is that at temperatures below 2.1 K there does exist an efficient coupling between the crystal and the helium bath such that the resonant phonons appear to pass freely into the helium bath. Above 2.1 K, the thermal coupling breaks down and the crystal is overheated.

V. SUMMARY

Each trap in the TCB lattice was shown to select a band of phonons within the black body spectrum of the heater radiation which corresponded to the trap depth below the host exciton band. The manifestation of this phenomenon was the particular power dependence associated with the phosphorescence modulation depth for each trap. Although there was a fairly large spread in the fitting parameter B, the spread in the effective heater temperature was considerably smaller, since $T_H \propto (P/B)^{1/4}$. Therefore, the results were consistent with the notion that the phonon spectrum can be characterized by an effective heater temperature common to all the experiments. It thus follows that the frequency spectrum of the phonon flux is also not appreciably shifted by scattering processes in the bulk of the thin crystal slabs.

The main emphasis of this work was to show that the heat pulse technique can be used to provide information with regard to the parameters governing phonon interactions in molecular solids. The depletion of the trap population during the heat pulse did in fact show a dependence on the density of available band states as well as a sensitivity to the nature of the trap. Although the problem of trap-to-band energy transfer still requires much more attention, the study of heat pulses in molecular crystals should be extended to other interesting problems. One such area would be that of exciton-phonon scattering in a wide-band system such as 1,4-dibromonaphthalene.

Acknowledgments

The authors would like to thank Prof. A. H. Francis for his generous gift of the thin-film heaters and particularly the late Professor V. L. Broude for many stimulating conversations during his recent visit to the United States. This work was supported in part by a grant from the National Science Foundation, and in part by the Materials and Molecular Research Division, Division of Chemical Sciences, Office of Basic Energy Sciences, U.S. Department of Energy under Contract No. W-7405-Eng-48.

References

1. J. Frenkel, *Phys. Rev.*, **37**, 17, 1276 (1931).
2. A. S. Davydov, *Theory of Molecular Excitons* (New York: McGraw-Hill, 1962).
3. G. F. Koster and J. C. Slater, *Phys. Rev.*, **95**, 1167 (1954).
4. M. D. Fayer and C. B. Harris, *Phys. Rev.*, **B9**, 748 (1974); *Chem. Phys. Lett.*, **25**, 149 (1974).
5. G. C. Nieman and G. W. Robinson, *J. Chem. Phys.*, **37**, 2150 (1962); **39**, 1298 (1963).
6. M. T. Lewellyn, A. H. Zewail, and C. B. Harris, *J. Chem. Phys.*, **63**, 3687 (1975).
7. R. M. Shelby, A. H. Zewail, and C. B. Harris, *J. Chem. Phys.*, **64**, 3192 (1976).
8. S. J. Hunter, H. Parker, and A. H. Francis, *J. Chem. Phys.*, **61**, 1390 (1974).
9. A. I. Attia, B. H. Loo, and A. H. Francis, *J. Chem. Phys.*, **61**, 4527 (1974).
10. R. J. von Gutfeld and A. H. Nethercot, *Phys. Rev. Lett.*, **12**, 641 (1964).
11. R. J. von Gutfeld, in *Physical Acoustics*, ed. by W. Mason (New York: Academic Press, 1969), vol. V, pp. 233–289.
12. V. L. Broude, N. A. Vidmont, V. V. Korshunov, I. B. Levinson, A. A. Maksimov, and I. I. Tartakovskii, *JETP Lett.*, **25**(6), 262 (1977).
13. V. L. Broude, N. A. Vidmont, D. V. Kazakovtsev, V. V. Korshonov, I. B. Levinson, A. A. Maksimov, I. I. Tartakovskii, and V. P. Yashnikov, *Sov. Phys. JETP*, **47**(1), 161 (1978).
14. C. H. Anderson and E. S. Sabisky, in *Physical Acoustics*, ed. by W. Mason (New York: Academic Press, 1971), vol. VIII, pp. 1–57.
15. O. Weis, *Z. Angew. Physik*, **26**, 325 (1969).
16. P. Herth and O. Weis, *Z. Angew. Physik*, **29**, 101 (1970).

17. W. A. Little, *Can. J. Phys.*, **37**, 334 (1959).
18. R. Berman, *Cryogenics*, **3**, 215 (1963).
19. P. Klemens, in *Thermal Conductivity*, ed. by R. Tye (London: Academic Press, 1969), vol. 1, pp. 1–68.
20. R. Berman, *Thermal Conduction in Solids* (Oxford: Clarendon Press, 1976), pp. 73–103.
21. C. Walter and R. Pohl, *Phys. Rev.*, **131**, 1433 (1963).
22. A. R. Burns, Ph.D. Thesis, University of California, Berkeley (1978).
23. Chorng-Jee Guo and Humphrey J. Maris, *Phys. Rev. Lett.*, **29**, 855 (1972); *Phys. Rev.*, **A10**, 960 (1974).
24. T. J. B. Swanenburg and J. Wolter, *Phys. Rev. Lett.*, **31**, 693 (1973).
25. L. J. Challis, *J. Phys. C: Solid State Physics*, **7**, 481 (1974).
26. M. Fooladi, U.S. Patent 3,557,227 (1971).
27. The 98.6% d_2-TCB material was originally prepared by J. C. Brock: the 99.1% material was furnished by M. D. Fayer.
28. A. H. Francis and C. B. Harris, *J. Chem. Phys.*, **57**, 1050 (1972).
29. D. D. Dlott and M. D. Fayer, *Chem. Phys. Lett.*, **41**, 305 (1976).
30. M. J. Buckley and A. H. Francis, *Chem. Phys. Lett.*, **23**, 582 (1973).
31. A. I. Attia, M. J. Buckley, R. M. Panos, and J. M. Raney, *Phys. Rev.*, **B15**, 1239 (1977).
32. Hans Glättli, *Can. J. Phys.*, **46**, 103 (1968).